RSC Advances

PAPER

View Article Online
View Journal | View Issue

Cite this: *RSC Adv.*, 2019, **9**, 7251

Ochrasperfloroid, an ochratoxin–ergosteroid heterodimer with inhibition of IL-6 and NO production from *Aspergillus flocculosus* 16D-1†

Bin-Bin Gu, Fu-Rong Jiao, Wei Wu, Lei Liu, Wei-Hua Jiao, Fan Sun, Shu-Ping Wang, Fan Yang and Hou-Wen Lin *

Received 24th December 2018
Accepted 18th February 2019

DOI: 10.1039/c8ra10539a

rsc.li/rsc-advances

A novel ochratoxin–ergosteroid heterodimer, ochrasperfloroid (**1**), together with a known mycotoxin, ochratoxin A (**2**), were isolated from the sponge-derived fungus *Aspergillus flocculosus* 16D-1. The structure of **1** was determined on the basis of 1D/2D NMR, HRESIMS/MS, and LC-UV/MS analysis of its alkaline hydrolyzates, quantum-chemical ^{13}C NMR calculation, and comparison with literature data. Of note, the ergosteroid embedded in **1** is also a new structure. Ochrasperfloroid (**1**) showed potent inhibitory activity towards IL-6 production in lipopolysaccharide (LPS)-induced THP-1 cell line, with an IC_{50} value of 2.02 μM, and NO production in LPS-activated RAW264.7 macrophages, with an IC_{50} value of 1.11 μM.

Introduction

Inflammatory responses play critical roles in cancer development and progression, including tumor initiation, promotion, progression, and metastasis.[1–6] Interleukin-6 (IL-6) and nitric oxide (NO) can be expressed at high levels in the tumor microenvironment and are now recognized as important mediators linking inflammation and cancer.[1–10] Therefore, IL-6 and NO are promising therapeutic and preventive targets as well as prognostic factors for cancer.[1–6,8–10]

In recent years, marine-derived fungi have been attracting ever-increasing attention as a promising reservoir for new biologically and pharmaceutically active marine natural products (MNPs) and have risen to the third-largest source of MNPs.[11–15] Sponge-derived fungi, as fungi with unique habitat, represent an important fountainhead of novel bioactive MNPs for drug discovery.[11–14,16] In our continuous endeavor to search for potential immunomodulatory MNPs,[17–19] the metabolites produced by *Aspergillus flocculosus* 16D-1, a fungus isolated from the inner tissue of the sponge *Phakellia fusca*, were analyzed. The EtOAc extract displayed inhibitory activity against IL-6 production in lipopolysaccharide (LPS)-induced THP-1 cell line and NO production in LPS-activated RAW264.7 macrophage cells. Subsequent separation and purification of the extract resulted in the discovery of ochrasperfloroid (**1**), a novel ochratoxin–ergosteroid heterodimer, and ochratoxin A (**2**),[20] one of the most-abundant food-contaminating mycotoxins (Fig. 1). It is noteworthy that the ergosteroid embedded in **1** is also a new structure. Herein, we report the isolation, structure elucidation, and biological evaluation of compounds **1** and **2**.

Results and discussion

Ochrasperfloroid (**1**) was evidenced to have a molecular formula of $C_{48}H_{58}NO_{14}Cl$ with 20 degrees of unsaturation, based on its $[M - H]^-$ molecular ion at *m*/*z* 906.3483 in the HRESIMS. The IR spectrum displayed absorptions for hydroxy (3380 cm^{-1}) and carbonyl (1751, 1679 cm^{-1}) groups. The ^1H NMR and HSQC spectra (Table 1) showed 18 methines, which include eight oxygenated/aminated methines (δ_H 5.62, 5.06, 4.85, 4.75, 4.01, 4.00, 3.47, 3.14) and six aromatic methines (δ_H 8.06, 7.36, 7.36,

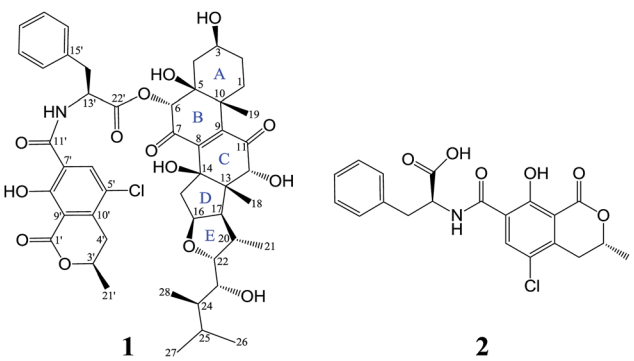

Fig. 1 Structures of **1** and **2**.

Key Laboratory for Marine Drugs, Department of Pharmacy, State Key Laboratory of Oncogenes and Related Genes, Renji Hospital School of Medicine, Shanghai Jiao Tong University, Shanghai 200127, China. E-mail: franklin67@126.com

† Electronic supplementary information (ESI) available: 1D and 2D NMR, HRESIMS, HRESIMS/MS, UV, IR, and ECD spectra of compound **1** and ^1H and ^{13}C NMR spectra of compound **2**; full details of computational method for quantum-chemical ^{13}C NMR calculation; table of ^1H and ^{13}C NMR spectroscopic data of compound **2**. See DOI: 10.1039/c8ra10539a

Table 1 ^{1}H (600 MHz) and ^{13}C (150 MHz) NMR data of **1** in DMSO-d_6, coupling constants in Hz (in brackets)

Position	δ_C, type	δ_H (J in Hz)	Position	δ_C, type	δ_H (J in Hz)
1	23.1, CH_2	α2.18, brd (14.3)	26	15.6, CH_3	0.70, d (6.8)
		β1.89, td (14.3, 3.2)	27	21.8, CH_3	0.86, d (6.9)
2	29.2, CH_2	α1.33[a], m	28	10.0, CH_3	0.67, d (6.9)
		β1.50[a], m	12-OH		6.28, d (4.3)
3	64.4, CH	4.01[a], m	1′	168.3, C	
4	31.8, CH_2	α1.32, brd (14.1)	3′	75.4, CH	4.85, m
		β1.97, brd (14.1)	4′	31.6, CH_2	3.23[a], dd (17.3, 3.3)
5	75.1, C				2.91, dd (17.3, 11.7)
6	78.5, CH	5.62, s	5′	121.5, C	
7	193.7, C		6′	136.0, CH	8.06, s
8	145.5, C		7′	120.1, C	
9	146.8, C		8′	158.3, C	
10	44.2, C		9′	111.3, C	
11	202.5, C		10′	141.7, C	
12	82.1, CH	3.47, d (4.3)	11′	163.0, C	
13	54.7, C		12′-NH		8.65, d (8.0)
14	80.7, C		13′	53.7, CH	5.06, td (8.0, 5.0)
15	49.6, CH_2	2.27, m	14′	36.8, CH_2	3.21[a], dd (14.0, 8.4)
16	85.0, CH	4.75, td (7.4, 2.5)			3.36, dd (14.0, 5.0)
17	58.7, CH	2.32, t (7.4)	15′	136.6, C	
18	15.14, CH_3	0.93, s	16′	129.4, CH	7.36, d (7.4)
19	22.7, CH_3	1.48, s	17′	128.3, CH	7.29, t (7.4)
20	38.7, CH	2.64, m	18′	126.7, CH	7.22, t (7.4)
21	15.08, CH_3	1.04, d (6.9)	19′	128.3, CH	7.29, t (7.4)
22	81.6, CH	4.00[a], dd (7.8, 1.7)	20′	129.4, CH	7.36, d (7.4)
23	72.7, CH	3.14, dd (9.1, 1.7)	21′	20.1, CH_3	1.47, d (6.3)
24	40.3, CH	1.56, m	22′	170.2, C	
25	25.5, CH	2.10, m	8′-OH		12.61, s

[a] Overlapped with other signals.

7.29, 7.29, 7.22), six methylenes (δ_H 3.21, 3.36; 3.23, 2.91; 2.27; 2.18, 1.89; 1.32, 1.97; 1.33, 1.50), and seven methyls (δ_H 1.48, 1.47, 1.04, 0.93, 0.86, 0.70, 0.67). According to the molecular formula, the remaining seven hydrogens are due to the presence of seven exchangeable protons in the molecule, three of which are visible in the ^{1}H NMR spectrum (δ_H 12.61, 8.65, 6.28). Its ^{13}C NMR and DEPT spectra (Table 1) manifested a total of 48 carbon resonances divided into 19 sp^2 carbon atoms [six methine carbons and 13 nonprotonated carbons, five of which are carbonyl carbons (δ_C 202.5, 193.7, 170.2, 168.3, 163.0)] and 29 sp^3 carbon atoms (four nonprotonated carbon atoms, 12 methine, six methylene, and seven methyl carbon atoms), accounting for 12 degrees of double-bond equivalents. The remaining eight degrees of unsaturation are due to the presence of eight rings in the molecule.

The ^{1}H and ^{13}C NMR spectroscopic data of **1** at positions 1′−22′ are almost the same as those of **2** (Tables 1 and S3†), indicating the presence of substructure **A** in **1** (Fig. 2), which was confirmed by analysis of the COSY and HMBC data.

Methine H-22 (δ_H 4.00) showed two-bond connectivity to C-23 (δ_C 72.7) and three-bond correlation to C-16 (δ_C 85.0). Methyl H_3-28 (δ_H 0.67) exhibited three-bond coupling to C-25 (δ_C 25.5). These HMBC correlations together with COSY determined spin systems H_2-15/H-16/H-17/H-20 (H-20/H_3-21)/H-22, H-23/H-24/H_3-28, and H_3-26/H-25/H_3-27 were sufficient in generating the E ring and its exocyclic C-22 alkanol side chain (Fig. 2). H_3-18 (δ_H 0.93) showed three-bond correlations to C-12 (δ_C 82.1), C-14 (δ_C 80.7), and C-17 (δ_C 58.7) and two-bond correlation to C-13 (δ_C 54.7) and H_2-15 (δ_H 2.27) showed three-bond correlations to C-13 and C-8 (δ_C 145.5) and two-bond correlation to C-14, constructing the D ring and its C-14-connected olefinic carbon C-8 and C-13-connected oxygenated

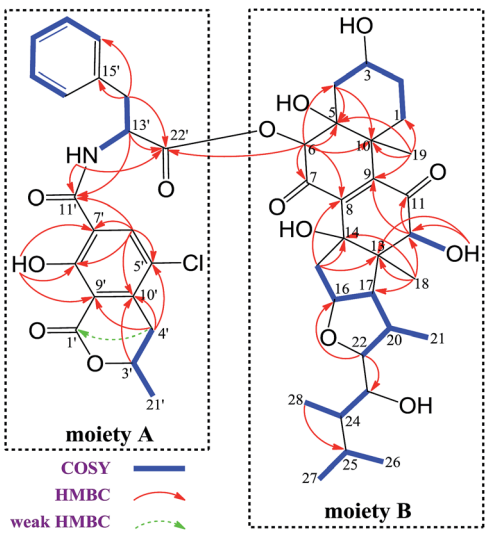

Fig. 2 Key COSY and HMBC correlations of **1**.

methine carbon C-12. A consecutive COSY correlations, H_2-1/H_2-2/H-3/H_2-4, coupled with HMBC correlations from H-4β (δ_H 1.97) to C-5 (δ_C 75.1) and C-10 (δ_C 44.2), from H_3-19 (δ_H 1.48) to C-1 (δ_C 23.1), C-5, C-9 (δ_C 146.8), and C-10, and from H-6 (δ_H 5.62) to C-4 (δ_C 31.8), C-5, and C-10 corroborated the presence of ring A and its C-5-connected oxygenated methine carbon C-6 (δ_C 78.5) and C-10-connected olefinic carbon C-9 (Fig. 2). In addition, an HMBC correlation from H-6 to C-22′ (δ_C 170.2) indicated an ester linkage between moiety **A** and C-6.

Moiety **A** accounts for two exchangeable protons, which leaves five exchangeable protons unassigned in substructure **B**. Accordingly, oxygenated carbons C-3 (δ_C 64.4), C-5, C-12, C-14, and C-23 in subunit **B** must be hydroxy-anchored carbons. Then it only remained to assign two carbonyls, C-7 (δ_C 193.7) and C-11 (δ_C 202.5), and to construct the last two rings in substructure **B**. As C-8 and C-9 are the only two olefinic carbons in compound **1**, they must be connected directly. On the basis of geometric considerations and HMBC correlations of H-6/C-7, H-6/C-8, H-12 (δ_H 3.47)/C-9, and H-12/C-11, it could only be explained by inserting carbonyl C-7 between C-6 and C-8, generating ring B, and inserting carbonyl C-11 between C-9 and C-12, constructing ring C (Fig. 2). The assignments were further confirmed by the HRESIMS/MS fragment ion series at *m*/*z* 386.0804 $[M + H]^+$, 404.0905 $[M + H]^+$, 358.0853 $[M + H]^+$, 239.0113 $[M + H]^+$, 402.0737 $[M - H]^-$, 521.2751 $[M - H]^-$, and 384.0630 $[M - H]^-$ (Fig. 3).

The identity of moiety **A** as shown (Fig. 1) was substantiated by LC-UV/MS analysis the base hydrolysates of **1** (Fig. 4), wherein peak a has the same retention time, *m*/*z* ratio, and M + 2 isotope pattern as **2**, and by comparison the specific rotation of the re-purified compound "peak a" ($[\alpha]_D^{25}$ −58.0 (*c* 0.4, MeOH)) with that of **2** ($[\alpha]_D^{25}$ −60.0 (*c* 0.4, MeOH)).[21]

We then tried to establish the relative configurations of 13 stereogenic centers (C-3, C-5, C-6, C-10, C-12, C-13, C-14, C-16, C-17, C-20, C-22, C-23, and C-24) in moiety **B** (Fig. 2). Nevertheless, rings A/B and C/D/E are segregated by an unsaturated ketone segment (C-7/C-8/C-9/C-11), which means that the relaying of configurational assignment from A/B to C/D/E is cut off. Therefore, the relative configurations of rings A/B and C/D/E were assigned separately (Fig. 5).

The ROESY correlation Me-19/H-6 revealed the relative configurations of C-6 and C-10 (6*R** and 10*R**; Fig. 5a, **A1**).

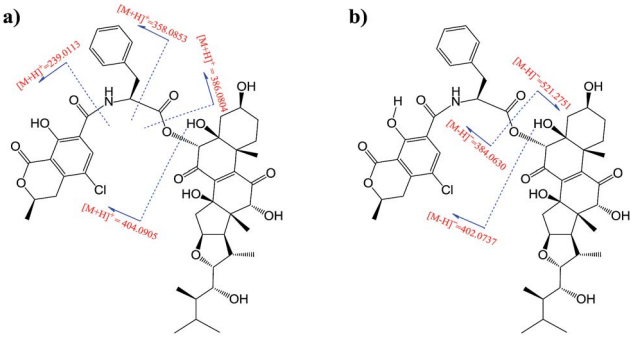

Fig. 3 HRESIMS/MS fragment ions (*m*/*z*) of **1**. (a) Positive ion mode; (b) negative ion mode.

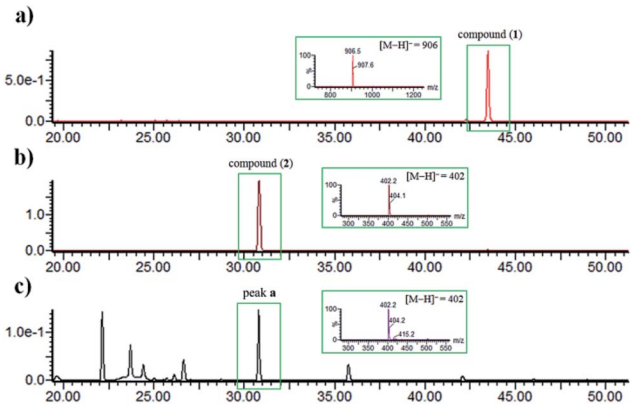

Fig. 4 LC-UV/MS chromatograms. (a) Standard compound **1**; (b) standard compound **2**; (c) EtOAc extract of the hydrolysis product of pure compound **1** in sodium hydroxide (2 M). The MS spectra of the peaks with green frame are shown in the insets (negative ionization mode).

However, no evidence existed from which the relative configurations of C-3 and C-5 could be determined directly. Regardless of the configuration of C-3, there have two candidate stereoisomers (**A1** and **A2**) for unit A/B (Fig. 5a and b), and only **A1** satisfied the ROESY correlations observed on rings A/B, as shown in the molecular modeling simulation, by which the relative configuration of C-5 (5*S**) was revealed. Next, the ROESY cross-peaks of H-3/H-2α, H-3/H-2β, H-3/H-4α, and H-3/H-4β uncovered the 3*S** configuration for C-3 (Fig. 5a, **A1**).

The relative configurations of C-12, C-13, C-16, C-17, C-20, and C-22 (12*R**, 13*S**, 16*S**, 17*R**, 20*S**, and 22*R**) in rings C/

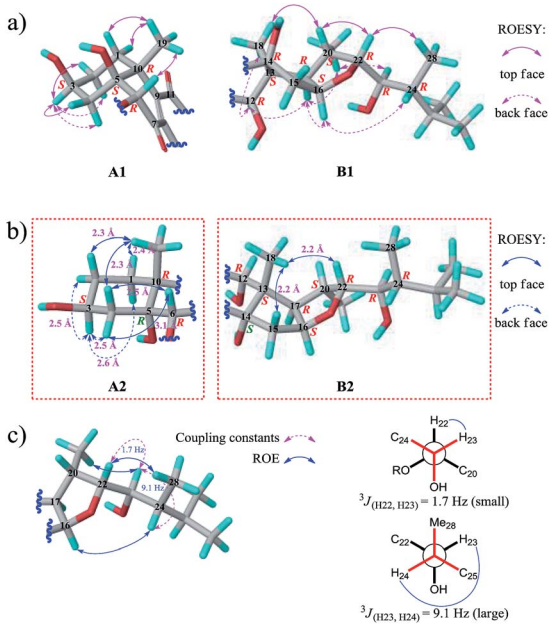

Fig. 5 (a) Key ROESY correlations of **1** (**A1**, rings A/B; **B1**, rings D/E). (b) The expected ROESY correlations on the structures of C-5 epimer of **1** (**A2**, rings A/B) and C-14 epimer of **1** (**B2**, rings D/E). (c) Relative configuration of the C-22 alkanol side chain of **1** determined by one- and two-dimensional NMR analysis (solid arrows, selected ROE correlations; dashed arrows, coupling constants).

D/E were unmasked by "top face" correlations H-20/Me-18 and H-20/H-22 and "back face" correlations Me-18/H-12, H-17/H-12, H-17/H-16, and H-17/Me-21 (Fig. 5a, **B1**). As the situation described above, the remaining one stereogenic center C-14 in unit C/D/E led to two candidate stereoisomers **B1** and **B2** (Fig. 5a and b), and only **B1** was in line with the ROESY correlations observed. Thus, the relative configuration of C-14 was ascertained to be 14*R** (Fig. 5a, **B1**). The relative configurations of C-23 and C-24 on the alkanol side chain were determined to be 23*R** and 24*R** by conformational analysis, based on ROESY correlations Me-21/H-23, H-22/Me-28, and H-16/H-24 and coupling constants $^{3}J_{H22\text{-}H23}$ and $^{3}J_{H23\text{-}H24}$ (Fig. 5c), which can also be supported by the fact that the chemical shifts of the C-22 alkanol side chain of **1** are nearly the same as that of asperflosterol,[19] which was previously isolated from the same fungus.

As compound **1** and asperflosterol[19] are derived from the same fungus and they have the same relative configurations at C-3, C-5, C-10, C-12, C-13, C-14, C-16, C-17, C-20, C-22, C-23, and C-24, which was supported by ^{13}C NMR chemical shifts calculation of the analogue of moiety **B** (model **I**, CMAE = 1.9 ppm, RMSD = 2.2 ppm, R^2 = 0.9983; see Fig. 6 and Table S2†),[22] we assigned the absolute configuration of moiety **B** as shown (Fig. 1). Thus, the structure of **1** was established with its absolute configuration. Since compound **1** is a heterodimer containing ochratoxin A (**2**), which is connected by an ester linkage to a new ergosteroid in **1**, it is possible that **1** was formed as an artifact during the extraction and isolation procedure.

Compounds **1** and **2** were evaluated for their inhibitory effects on IL-6 production in LPS-induced THP-1 cells and NO production in LPS-activated RAW264.7 macrophages. As shown in Table 2, compound **1** showed potent inhibitory activities against IL-6 and NO productions with IC_{50} values of 2.02 and 1.11 μM, respectively, whereas compound **2** exhibited no inhibitory effects on IL-6 and NO productions (IC_{50} > 25 μM). An CCK-8 assay was carried out to determine whether the suppressive effects were related to cell viability, but no cytotoxicities against THP-1 and RAW264.7 cells were detected (IC_{50} > 20 μM), suggesting that the inhibitory activities towards IL-6 and NO productions did not involve general cytotoxicity. In addition, cytotoxic activity against A549 and HepG2 cell lines was performed, indicating that **1** and **2** displayed weak to medium cytotoxic activity against these two tumor cell lines with IC_{50} values of 55.0 and 50.3 μM for A549 cells and 23.6 and 22.7 μM for HepG2 cells, respectively.

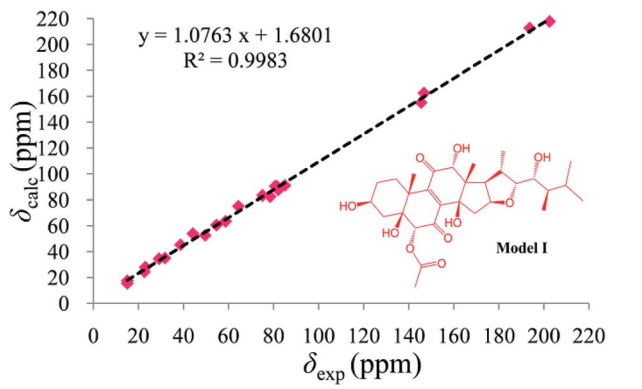

Fig. 6 Regression analysis of experimental ^{13}C NMR chemical shifts of moiety **B** in **1** *versus* calculated ^{13}C NMR chemical shifts of model **I** at b3lyp/6-311 + g(2d,p) PCM (DMSO) level; linear fitting is shown as a line. The structure of model **I** is shown in the inset.

Table 2 Determination of mitigation of IL-6 production in induced THP-1 cells and NO production in activated RAW264.7 cells [given as IC_{50} (μM)]

Compound	IL-6	NO
1	2.02	1.11
2	>25	>100
Corylifol A[a]	0.88	
Diphenyleneiodonium chloride[b]		0.06

[a] Positive control for inhibition of IL-6 production. [b] Positive control for inhibition of NO production.

Conclusions

A novel ochratoxin–ergosteroid heterodimer, ochrasperfloroid (**1**), along with a known mycotoxin, ochratoxin A (**2**), were isolated from the sponge derived fungus *A. flocculosus* 16D-1. **1** showed significant inhibitory effects on IL-6 production in LPS-induced THP-1 cells and NO production in LPS-activated RAW264.7 cells, whereas **2** showed no inhibitory effects on IL-6 and NO productions. Besides, **1** and **2** showed weak to medium cytotoxic activity against A549 and HepG2 cell lines. Although the EtOAc extract of *A. flocculosus* 16D-1 was thoroughly checked and isolated, we did not find the new ergosteroid that embedded in **1**. Moreover, acid or alkaline hydrolysis of **1** didn't afford the ergosteroid as well. Therefore, it is challenging to address the detailed structure–bioactivity relationship of **1** and **2**.

Experimental section

General procedures

Optical rotation measurements were carried out on a PerkinElmer model 341 polarimeter with a 10 cm length cell at room temperature. IR and UV spectra were recorded on a Bruker tensor 27 FTIR spectrometer and a Hitachi U-3010 spectrophotometer, respectively. ECD spectra were obtained from a Jasco J-715 spectropolarimeter. ^{1}H, ^{13}C, DEPT135, COSY, HSQC, HMBC, and ROESY NMR spectra were collected on an Agilent 600 MHz NMR apparatus. Chemical shifts (δ) are referenced to tetramethylsilane (TMS) at 0.00 ppm and the residual solvent peak of DMSO-d_6 at 39.52 ppm, for proton and carbon, respectively. HRESIMS and HRESIMS/MS spectra were determined on a Waters Xevo G2-XS QTOF spectrometer. HPLC-MS spectra were collected using a Waters HPLC system equipped with a Waters Acquity QDa spectrometer and a Waters XBridge C18 column (4.6 × 250 mm, 5 μm). Analytical thin-layer chromatography (TLC) systems were performed on silica gel 60 F_{254} plates. Column chromatography was performed using

silica gel 60 (200–300 mesh; Yantai). Preparative MPLC was carried out on an Interchim Puriflash 450 apparatus. Semi-preparative reversed-phased HPLC (RP-HPLC) was carried out using a Waters 1525 pump equipped with a 2998 photodiode array detector and a Waters XBridge C18 column (10 × 250 mm, 5 μm).

Fungal material

The fungus *A. flocculosus* 16D-1 was isolated from the inner tissue of the sponge *Phakellia fusca* collected from Yongxing Island, China. The specific name was identified according to its ITS rDNA sequences (GenBank accession no. KM605191). A voucher specimen of this fungus was deposited at the School of Life Sciences and Biotechnology, Shanghai Jiao Tong University, Shanghai, China.

Culture, extraction, and isolation

The strain was initially activated on PDA medium in a Petri dish for 7 days. Afterwards, its spores were directly inoculated into 250 mL Erlenmeyer flasks each containing 100 mL of the seed medium (dextrose 20 g L^{-1}, potato starch 200 g L^{-1}, and artificial seawater salts 30 g L^{-1} in purified H_2O) on a rotary shaker with 180 rpm at 28 °C for 72 h. The subsequent amplified fermentation was carried out in 120 × 2 L Erlenmeyer flasks. Each flask contained 80 g of rice, 120 mL of distilled H_2O, and 2 g artificial seawater salts, where 20 mL of the seed culture was transferred and incubated under static conditions at 25 °C for 40 days. The fermented substrate was exhaustively extracted with EtOAc, affording 56 g of extract after evaporating the solvent under reduced pressure. The extract (56 g) was subjected to column chromatography (CC) on silica gel, eluting with a CH_2Cl_2/MeOH gradient system (from 150 : 1 to 0 : 1), to afford 12 fractions (Fr.1-12). Fr.12 (1.38 g) was subjected to reversed-phase ODS MPLC (10–100% MeOH/H_2O, flow rate 20 mL min^{-1}, 180 min, UV detection at 210 nm) to give nine subfractions (Fr.12-1–Fr.12-9). Next, the subfraction Fr.12-7 (430 mg) was separated by semipreparative reversed-phase HPLC [Waters XBridge C18 column (10 × 250 mm, 5 μm), 60% MeCN/H_2O (0.1% formic acid), 2.0 mL min^{-1}, UV detection at 330 nm] to yield ochratoxin A (**2**, 100 mg, t_R 20.5 min). Fr.3 (8.26 g) was subjected to reversed-phase ODS MPLC (10–100% MeOH/H_2O, flow rate 20 mL min^{-1}, 180 min, UV detection at 210 nm) to yield 39 subfractions (Fr.3-1–Fr.3-39). Subfraction Fr.3-30 (150 mg) was then separated by semipreparative reversed-phase HPLC [Waters XBridge C18 column (10 × 250 mm, 5 μm), 87% MeOH/H_2O, 2.0 mL min^{-1}, UV detection at 330 nm] to yield ochrasperfloroid (**1**, 27.7 mg, t_R 15.4 min).

Ochrasperfloroid (1). Light yellow oil; $[\alpha]_D^{25}$ +23 (*c* 0.9, MeOH); UV (MeOH) λ_{max} (log ε) 200 (5.04), 330 (3.83) nm; IR (film) ν_{max} 3380, 3066, 2956, 1751, 1679, 1611, 1531, 1426, 1385, 1366, 1304, 1271, 1212, 1173, 1138, 1112, 1059, 1032, 992 cm^{-1}; ECD (7.87×10^{-4} M, MeOH), λ_{max} ($\Delta\varepsilon$) 200 (12.83), 231 (−8.13), 269 (5.77), 345 (−1.13), 413 (0.48) nm; ^1H and ^{13}C NMR data (DMSO-d_6), Table 1; HRESIMS *m*/*z* 906.3483 $[M - H]^-$ (calcd for $C_{48}H_{57}NO_{14}Cl$, 906.3468).

Ochratoxin A (2). White powder; $[\alpha]_D^{25}$ −60.0 (*c* 0.4, MeOH); ^1H and ^{13}C NMR data (DMSO-d_6), Table S3;† HRESIMS *m*/*z* 404.0913 $[M + H]^+$ (calcd for $C_{20}H_{19}NO_6Cl$, 404.0901).

Cytotoxicity assay

The cytotoxic activities of compounds **1** and **2** towards THP-1, RAW264.7, A549, and HepG2 cell lines were assessed by the CCK-8 method as described previously.[23] Doxorubicin (0.80, 3.40, 0.13, and 0.06 μM, respectively) was used as positive control.

IL-6 immune-suppressive activity assay

The IL-6 immune–suppressive activity of compounds **1** and **2** was evaluated according to the method described by Chen *et al.*[24] Corylifol A was used as positive control.[25]

Nitric oxide inhibitory activity assay

The NO inhibitory activity of compounds **1** and **2** was assessed with the method described previously.[26] Diphenyleneiodonium chloride was used as positive control.[27]

Conflicts of interest

There are no conflicts of interest to declare.

Acknowledgements

This project is financially supported by National Key Research and Development Program of China (2018YFC0310900), National Natural Science Fund of China (No. 41476121, U1605221, 21502113, 41576130, 81502936, 81741151).

Notes and references

1 N. Unver and F. Mcallister, *Cytokine Growth Factor Rev.*, 2018, **41**, 10.
2 T. Tanaka, M. Narazaki and T. Kishimoto, *Cold Spring Harbor Perspect. Biol.*, 2014, **6**, a016295.
3 D. E. Johnson, R. A. O'Keefe and J. R. Grandis, *Nat. Rev. Clin. Oncol.*, 2018, **15**, 234.
4 Y. Guo, F. Xu, T. Lu, Z. Duan and Z. Zhang, *Cancer Treat. Rev.*, 2012, **38**, 904.
5 K. Taniguchi and M. Karin, *Semin. Immunol.*, 2014, **26**, 54.
6 C. A. Hunter and S. A. Jones, *Nat. Immunol.*, 2015, **16**, 448.
7 D. F. Quail and J. A. Joyce, *Nat. Med.*, 2013, **19**, 1423.
8 A. Maiuthed, N. Bhummaphan, S. Luanpitpong, A. Mutirangura, C. Aporntewan, A. Meeprasert, T. Rungrotmongkol, Y. Rojanasakul and P. Chanvorachote, *J. Biol. Chem.*, 2018, **293**, 13534.
9 H. Cheng, L. Wang, M. Mollica, A. T. Re, S. Wu and L. Zuo, *Cancer Lett.*, 2014, **353**, 1.
10 D. Basudhar, V. Somasundaram, G. A. de Oliveira, A. Kesarwala, J. L. Heinecke, R. Y. Cheng, S. A. Glynn, S. Ambs, D. A. Wink and L. A. Ridnour, *Antioxid. Redox Signaling*, 2017, **26**, 1044.
11 M. E. Rateb and R. Ebel, *Nat. Prod. Rep.*, 2011, **28**, 290.

12 J. W. Blunt, B. R. Copp, R. A. Keyzers, M. H. G. Munro and M. R. Prinsep, *Nat. Prod. Rep.*, 2016, **33**, 382.
13 J. W. Blunt, B. R. Copp, R. A. Keyzers, M. H. G. Munro and M. R. Prinsep, *Nat. Prod. Rep.*, 2017, **34**, 235.
14 J. W. Blunt, A. R. Carroll, B. R. Copp, R. A. Davis, R. A. Keyzers and M. R. Prinsep, *Nat. Prod. Rep.*, 2018, **35**, 8.
15 M. Saleem, M. S. Ali, S. Hussain, A. Jabbar, M. Ashraf and Y. S. Lee, *Nat. Prod. Rep.*, 2007, **24**, 1142.
16 U. Hentschel, J. Piel, S. M. Degnan and M. W. Taylor, *Nat. Rev. Microbiol.*, 2012, **10**, 641.
17 B.-B. Gu, W. Wu, L.-Y. Liu, J. Tang, Y.-J. Zeng, S.-P. Wang, F. Sun, L. Li, F. Yang and H.-W. Lin, *Eur. J. Org. Chem.*, 2018, **2018**, 48.
18 B.-B. Gu, F.-R. Jiao, W. Wu, W.-H. Jiao, L. Li, F. Sun, S.-P. Wang, F. Yang and H.-W. Lin, *J. Nat. Prod.*, 2018, **81**, 2275.
19 B.-B. Gu, W. Wu, F.-R. Jiao, W.-H. Jiao, L. Li, F. Sun, S.-P. Wang, F. Yang and H.-W. Lin, *Org. Lett.*, 2018, **20**, 7957.
20 L. Alanati and E. Petzinger, *J. Vet. Pharmacol. Ther.*, 2006, **29**, 79.
21 X. Xu, F. He, X. Zhang, J. Bao and S. Qi, *Food Chem. Toxicol.*, 2013, **53**, 46.
22 M. W. Lodewyk, M. R. Siebert and D. J. Tantillo, *Chem. Rev.*, 2012, **112**, 1839.
23 W.-Z. Tang, Z.-Z. Yang, F. Sun, S.-P. Wang, F. Yang and H.-W. Lin, *J. Asian Nat. Prod. Res.*, 2017, **19**, 691.
24 H. Chen, F. Wang, H. Mao and X. Yan, *Biochim. Biophys. Acta*, 2014, **1840**, 2162.
25 S. W. Lee, B. R. Yun, M. H. Kim, C. S. Park, W. S. Lee, H. M. Oh and M. C. Rho, *Planta Med.*, 2012, **78**, 903.
26 W.-H. Jiao, T.-T. Xu, F. Zhao, H. Gao, G.-H. Shi, J. Wang, L.-L. Hong, H.-B. Yu, Y.-S. Li, F. Yang and H.-W. Lin, *Eur. J. Org. Chem.*, 2015, **2015**, 960.
27 N. Srivastava, V. K. Gonugunta, M. R. Puli and A. S. Raghavendra, *Planta*, 2009, **229**, 757.